Journal of Electrical Engineering and Computer (JEECOM)
Vol. 8, No. 2 (2026), DOI: 10.33650/jeecom.v8i2.17162
p-ISSN: 2715-0410; e-ISSN: 2715-6427

Design of a Solar Charging Regulator Based on a Buck Converter that Integrates P&O PI MPPT Control and SOC Estimation Based on Coulomb Counting

Wildan Surya Wijaya [1*], Aditya Ilham [2], Dwi Hastuti [3], Maharani Wisudawati Swista [4], Alfiandi Aulia Rahmadani [5]

[1,2,3,4] Department of Electrical Engineering, University of PGRI Adi Buana Surabaya, Surabaya, Indonesia
[5] Department of Information and Communication Systems, Okayama University, Okayama 700-8530, Japan

Article Info

Article history:

Received August 25, 2026
Revised September 02, 2026
Accepted September 04, 2026

Keywords:

Photovoltaic
Perturb and Observe
Buck Converter
Coulomb Counting
State of Charge

ABSTRACT

Photovoltaic (PV) systems require an effective charging control strategy to regulate power transfer to batteries under varying operating conditions. This study develops and evaluates a simulation-based solar charging regulator that integrates a buck converter with Perturb and Observe (P&O) maximum power point tracking (MPPT), PI-based PV voltage regulation, and Coulomb Counting-based State of Charge (SOC) estimation. The proposed control structure combines MPPT for determining the PV voltage reference, a PI controller for regulating the PV voltage through buck converter duty-cycle adjustment, and a supervisory SOC control mechanism for managing the battery charging process. The system was modeled and simulated in MATLAB/Simulink to evaluate PV operating conditions, converter duty cycle, battery voltage and current, SOC estimation, and charging cut-off behavior. The simulation results show that the PV operating point is maintained at approximately 29 V and 7.5 A, corresponding to approximately 210 W during the initial charging condition. As the charging process progresses, the battery SOC increases from approximately 99.99% to 100% and reaches the defined full-charge condition at approximately 3.45 s. At the cut-off condition, the supervisory controller reduces the buck converter duty cycle from approximately 0.5 to 0, causing the battery charging current to decrease to 0 A and thus automatically disabling the charging command. These results demonstrate the feasibility of integrating P&O MPPT, PI-based voltage regulation, and Coulomb Counting-based SOC supervision into a coordinated solar charging regulator.

Corresponding Author:
Wildan Surya Wijaya,
Electrical Engineering Study Program, Universitas PGRI Adi Buana Surabaya, Surabaya, Indonesia
Email: wildansurya@unipasby.ac.id; Orchid Id: https://orcid.org/0009-0001-6502-0286

1. INTRODUCTION

Photovoltaic (PV) technology has significant potential as one of the renewable energy sources because it can be applied to various system scales. However, the power produced by PV is affected by environmental conditions, especially solar irradiation and temperature, so its current-current and voltage-power characteristics change and the PV operating point is not always at the maximum power point (Maximum Power Point, MPP). Therefore, the Maximum Power Point Tracking (MPPT) technique is used to maintain PV operations around MPP under various conditions [1], [2]. Various MPPT methods have been developed, such as Hill Climbing, Perturb and Observe (P&O), Incremental Conductance (INC), Fuzzy Logic Control (FLC), and Particle Swarm Optimization (PSO) [1], [3]. Among these techniques, P&O is widely used because its algorithm structure is simple and its computational requirements are relatively low [2], [4]. This method determines the direction of the change in the operating point by providing a perturbation to the PV voltage and observing the resulting power change. However, conventional P&O can experience oscillations around the MPP and performance degradation when environmental conditions change rapidly [2], [4], so that various P&O developments have been undertaken to improve tracking response [5]. Nonetheless, the main function of the MPPT is to optimize the PV operating point, so an additional mechanism is needed to determine whether the battery charging process can still be resumed when the charging condition has been reached.

In PV-based battery charging systems, DC–DC converters are used to regulate the energy transfer between PV and the battery. Buck converters are appropriately used when the PV voltage is higher than the battery charging voltage, while duty cycles are used to control the operating conditions of the converter. The integration of MPPT with DC–DC converters has been extensively studied to improve PV energy utilization and regulate power transfer during the charging process [6], [7]. Closed-loop controls, such as Proportional-Integral (PI), can be used to maintain voltage at reference values and improve the dynamic response of the system [8]. However, the setting of PV operating points and power transfer does not by itself provide information about the condition of the battery charge. For this reason, supervision parameters such as State of Charge (SOC) are required, which can be estimated using a variety of methods, including model-based methods, Kalman filters, and Coulomb Counting [9], [10]. Coulomb Counting calculates SOC changes based on the integration of battery current over time and is relatively simple to implement because it uses directly measured battery current [11], [12]. This method, however, is affected by the initial SOC, battery capacity uncertainty, current measurement errors, and the accumulation of integration errors [12].

Previous research has addressed MPPT, DC–DC converter control, and battery condition management from different approaches. Research [6], [8] develop a battery charging system that combines MPPT with DC–DC converter and charge control, so that PV power can be utilized and adjusted to the needs of battery charging. And research [9], [11] also developed PV systems with adaptive step-size P&O connected to buck converters and battery charging strategies. Meanwhile, research on SOC has focused more on the development and evaluation of estimation methods to obtain information on battery conditions, including the Coulomb Counting approach and filter-based methods [6], [7]. These studies show that MPPT, converter control, and battery condition monitoring have been extensively developed, but the focus of control is still different, namely PV power optimization, energy transfer regulation, or battery condition estimation. These differences in functions show the importance of regulating the relationship between the control parts when all three are used in a single PV-based battery charging system.

Although the integration of MPPT with converters and battery charging strategies has been developed in previous studies, the coordination between maximum power point tracking, converter regulation, and charging termination decisions based on battery condition still needs to be clarified. In some systems, MPPT plays a role in determining PV operating points, while converter controls are tasked with following these references through duty cycle settings. Meanwhile, SOC information is used to monitor battery condition, but it is not always placed as part of a monitoring mechanism that directly determines the sustainability of the charging process. These conditions indicate the need to distinguish the PV power optimization function and the charge monitoring function in a single coordinated control structure. In this study, P&O is used to generate PV voltage references, PI controllers set the duty cycle of the converter buck so that the PV voltage follows the reference, while Coulomb Counting is used to obtain SOC information that together with the battery voltage is the basis for the decision to maintain or stop charging commands. With this approach, the condition of the battery does not change the function of the MPPT, but becomes the basis for the supervisory controller to determine whether the charging process is still allowed.

The novelty of this research lies in the application of a hierarchical control structure that connects the process of tracking the maximum power of PV, the setting of the converter, and the monitoring of battery condition in a single charging system. In the proposed structure, the P&O is not only used to track the MPP, but also to generate the PV voltage reference which is input to the PI controller. The PI controller then adjusts the duty cycle of the buck converter so that the PV voltage follows the reference. At the supervisory level, Coulomb Counting is used to obtain SOC information which together with the battery voltage forms the basis for the decision to maintain or stop the charging process. With the division of functions, the condition of the battery can affect the charging permit without changing the main function of the MPPT in maintaining the PV operating point. The contribution of this research thus lies in the relationship and coordination between these levels of control in a single PV battery charging regulator architecture.

Therefore, this study aims to develop and evaluate a PV-based battery charge setting system using a buck converter that integrates P&O-based MPPT, PI-based PV voltage regulation, and Coulomb Counting-based SOC monitoring. In this structure, MPPT is used to maintain PV operations around the maximum power point, while the battery condition is used as the basis for determining whether the energy from PV can still be delivered to the battery. This strategy is used so that the process of extracting maximum power from PV does not directly cause charging to continue when the battery has reached the specified charging condition. Evaluations were carried out on PV voltage, current, and power, duty cycle buck converter, battery voltage and current, SOC response, and system response to the charging stop condition. The results of the evaluation were used to determine the system's ability to maintain the PV operating point, regulate energy transfer through the buck converter, monitor the battery charge condition, and stop the charge command when the SOC limit and the predetermined battery voltage were reached.

2. METHODS

This research uses a simulation-based method to design and evaluate a photovoltaic (PV) battery charging regulation system. The proposed system consists of a PV source, a buck converter, a battery, a Perturb and Observe (P&O) Maximum Power Point Tracking (MPPT) algorithm, a Proportional-Integral (PI) controller, and a Coulomb Counting-based State of Charge (SOC) estimation method. The buck converter serves as the power interface between the PV source and the battery [13], [14]. The P&O MPPT algorithm determines the reference PV voltage corresponding to the maximum power operating point, while the PI controller regulates the actual PV voltage by adjusting the converter duty cycle. Meanwhile, the Coulomb Counting method estimates the battery SOC and provides information to the supervisory control for determining the charging enable, cut-off, and restart conditions [15], [16].

The proposed system is modeled and simulated using MATLAB/Simulink. The simulation model is developed to evaluate the interaction between the MPPT algorithm, PI-controlled buck converter, battery charging process, and SOC-based supervisory control. The simulation results are evaluated based on the PV voltage, PV current, PV power, converter duty cycle, battery voltage, battery current, and estimated SOC [17].

The functional relationship among the PV source, P&O MPPT, PI controller, buck converter, battery, and Coulomb Counting-based SOC estimation is presented in Figure 1.

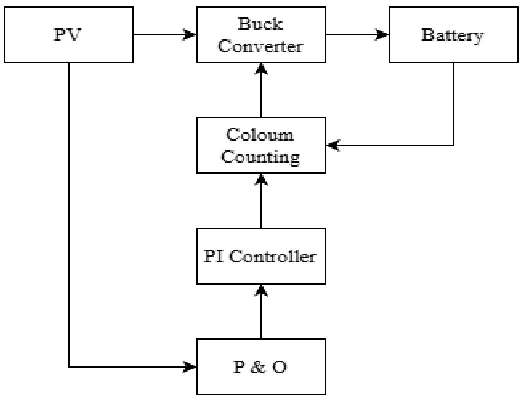

Figure 1. Block diagram of a solar charging control system based on a buck converter.

Figure 1 represents the conceptual control structure of the proposed system. The PV source provides voltage and current measurements to the P&O MPPT algorithm. Based on the measured PV voltage and power, the P&O algorithm determines the reference PV voltage. This reference is compared with the measured PV voltage, and the resulting error is processed by the PI controller. The PI controller generates the duty-cycle command for the buck converter so that the PV operating voltage follows the reference generated by the MPPT algorithm. The buck converter then transfers the PV-generated energy to the battery. At the battery side, the charging current is used by the Coulomb Counting method to estimate the SOC. The estimated SOC and battery voltage are subsequently provided to the supervisory control to determine whether the charging command remains enabled or is disabled.

The detailed implementation of the proposed control structure in the simulation environment is shown in Figure 2.

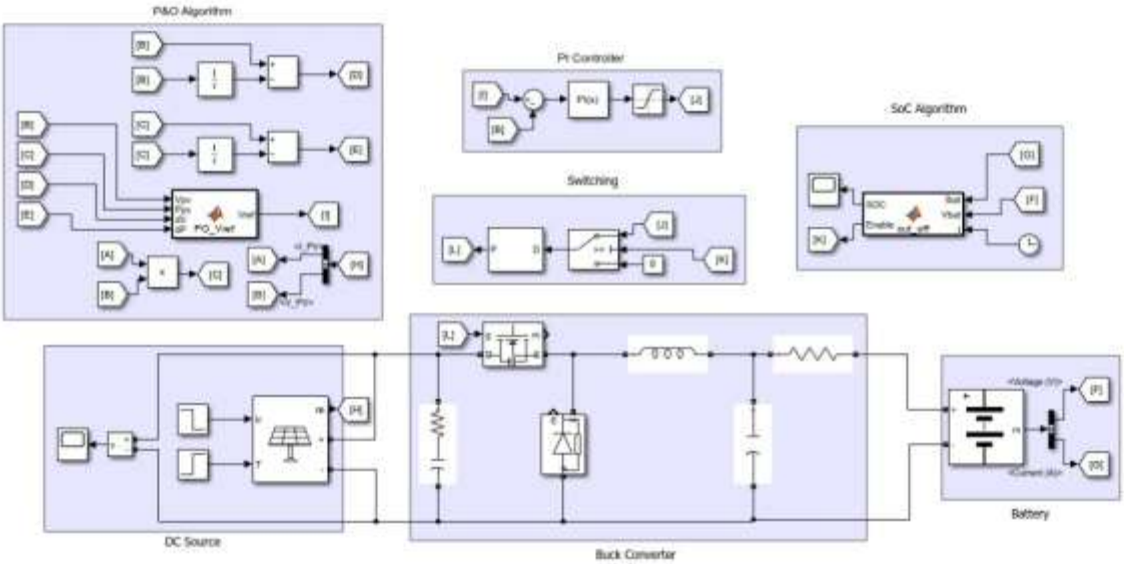

Figure 2. Overall configuration of a buck converter-based solar charging control system.

Figure 2 shows the overall simulation configuration used to implement the proposed system. It includes the signal connections between the PV model, P&O MPPT algorithm, PI controller, PWM generation, buck converter, battery model, SOC estimation, and switch. The detailed configuration allows the control sequence and signal flow used in the simulation to be evaluated.

2.1. Buck Converter

The buck converter is used as a step-down DC–DC converter that serves as an interface between the photovoltaic (PV) source and the battery. The converter reduces the PV voltage to a level suitable for the battery charging process. In addition to performing voltage conversion, the buck converter provides the control interface through which the PV operating point can be regulated. Changes in the converter duty cycle modify the electrical operating condition of the PV source, allowing the PV voltage to follow the reference generated by the Perturb and Observe (P&O) MPPT algorithm [18].

The buck converter circuit used in the proposed system is shown in Figure 3.

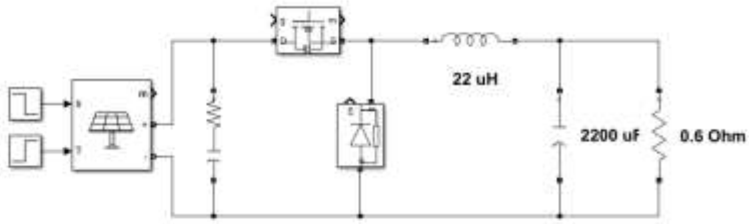

Figure 3. Buck converter circuit in a PV-based charging system.

The converter parameters are determined according to the operating conditions of the system. The design calculations include the duty cycle, inductor current ripple, output voltage ripple, average inductor current for rectifier diode selection, peak inductor current, inductance, capacitance, and load resistance. The calculated parameters are used as the basis for selecting and configuring the converter components in the simulation model [18].

The design equations used for the buck converter are summarized in Table 1.

Table 1. Buck Converter Formula.

No	Parameter		Nilai	
1	Duty Cycle	:	$D = \frac{Voutput\ buck}{Vinput}$	(1)
2	Ripple Current Inductor	:	$\Delta\, IL = 20\% x\, I_{output}$	(2)
3	Ripple Voltage	:	$\Delta\, Vout = 1\% xVin$	(3)
4	rectifier diode selection	:	$I_{L\ average\ Buck} = I_{out\ Buck}\ x\ (1 - dutty\ cycle)$	(4)

No	Parameter		Nilai	
5	Current Peak Inductor	:	$I_{peak\ buck} = I_{out\ Buck} + Delta_{IL}$	(5)
6	Inductor	:	$L = \frac{V_{out} \times (V_{in} - V_{out})}{\Delta I_L \times f_s \times V_{in}}$	(6)
7	Capacitor	:	$C = \frac{I_{output\ buck}{}^2 x\ Induktor\ buck}{2\ x\ V_{output\ buck} x\ Delta_{Vout\ Buck}}$	(7)
8	Recistor	:	$R_{load\ Buck} = \frac{V_{output}{}^2}{P}$	(8)

The table 1 presents several important parameters in the design of a buck converter, which are used to determine the specifications of the components and the characteristics of the circuit. Equation (1) is used to determine the *duty cycle* (D), which is the ratio of the output voltage (*Voutput*) to the input voltage (*Vinput*). The duty cycle indicates the proportion of time that the switch remains in the *ON* state during one switching period. Equation (2) is used to determine the *inductor ripple current* (ΔI_L), which is set at 20% of the output current (*Ioutput*). This value represents the allowable variation in the inductor current during the switching process. Equation (3) is used to determine the *output voltage ripple* (ΔV_{out}), which is set at 1% of the output voltage. This value represents the maximum allowable voltage variation to maintain a stable output voltage. Equation (4) is used for the selection of the rectifier diode by determining the average current flowing through the diode based on the output current and duty cycle, expressed as $I_{L\ average\ Buck} = I_{out}(1 - D)$. This equation indicates that the average diode current is affected by the duty cycle. Equation (5) is used to determine the peak inductor current (*Ipeak*), which is the sum of the output current and half of the inductor ripple current, $I_{peak} = I_{out} + \frac{\Delta I_L}{2}$. This value is important for ensuring that the selected inductor can handle the maximum current without reaching saturation.

Furthermore, Equation (6) is used to determine the required inductance value (L) for the buck converter. The inductance value is influenced by the input voltage, output voltage, allowable ripple current, switching frequency (f_s), and duty cycle. The inductor functions to store and release energy during the switching process, thereby maintaining a more stable output current. Equation (7) is used to determine the output capacitor value (*C*), which functions to reduce the *output voltage ripple*. The capacitor value is influenced by the output current, duty cycle, switching frequency, and allowable voltage ripple. A smaller target voltage ripple generally requires a larger capacitance value.

Finally, Equation (8) is used to determine the load resistance (R_{load}) based on the output voltage and load power, expressed as $R_{load} = \frac{V_{out}^2}{P}$. This equation shows the relationship between the output voltage, power consumed by the load, and load resistance. Therefore, Equations (1) through (8) are used as the basis for designing the buck converter, starting from determining the duty cycle, current and voltage ripple, and diode selection, to determining the peak current, inductor, capacitor, and load resistance values. The converter is configured to provide the required voltage and current conditions for charging the 12 V, 100 Ah lead-acid battery.

2.2. MPPT Perturb and Observe

The Perturb and Observe (P&O) algorithm is used to determine the maximum power point (MPP) operating condition of the photovoltaic (PV) source under varying irradiation conditions. The algorithm operates by applying a small perturbation to the PV reference voltage and observing the resulting change in PV power [19], [20]. Based on the change in power and voltage, the algorithm determines the direction of the next perturbation so that the PV operating point moves toward the maximum power point.

The P&O MPPT flowchart is shown in Figure 4.

ISSN: 2715-6427

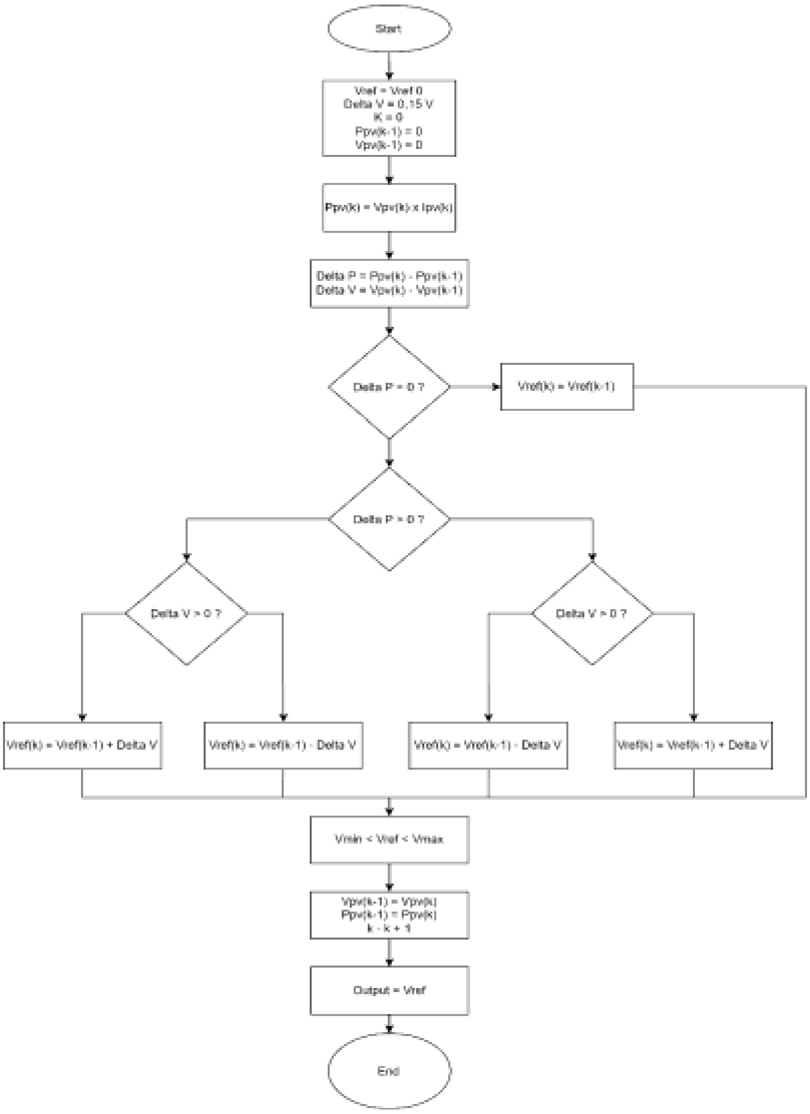

Figure 4. MPPT Perturb and Observe Flowchart.

As shown in Figure 4, the process begins by initializing the reference voltage, perturbation step size, and previous PV voltage and power values. The instantaneous PV power is then calculated from the measured PV voltage and current. The present power and voltage are compared with their corresponding values from the previous iteration to determine the direction of the perturbation. When the perturbation results in an increase in PV power, the perturbation direction is maintained. Conversely, when the PV power decreases, the perturbation direction is reversed.

In this study, the perturbation step is set to 0.15 V. After each update, the PV reference voltage is constrained within the predetermined operating range to maintain stable operation. The resulting reference voltage is then supplied to the PI controller. Therefore, the P&O algorithm determines the desired PV operating voltage, whereas the PI controller is responsible for regulating the actual PV voltage through the buck converter duty cycle. This control process is continuously repeated to respond to changes in the PV operating conditions.

2.3. PI Controller

The PI controller is used to regulate the PV operating voltage by controlling the duty cycle of the buck converter. The controller operates in a closed-loop configuration in which the reference PV voltage generated by the P&O MPPT algorithm is compared with the measured PV voltage. The resulting voltage error is processed by the PI controller to generate the duty-cycle command [21], [22].

The relationship between the reference voltage, measured PV voltage, PI controller, and converter duty cycle is illustrated in Figure 5.

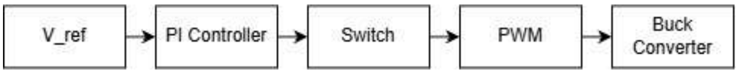

Figure 5. Duty cycle control block diagram.

The PI controller is implemented in parallel form and continuous-time representation. Its output is limited to the specified duty-cycle range to prevent the converter from operating outside the defined control limits. During normal charging, the PI controller output is passed through the supervisory switch to the PWM generator. The PWM signal then controls the switching device of the buck converter.

The supervisory switch provides an additional control layer for the battery charging process. When the battery has not reached the defined full-charge condition, the switch allows the PI-generated duty-cycle command to reach the PWM generator. When the cut-off condition is reached, the supervisory switch blocks the charging command and forces the PWM duty cycle to a non-charging condition. Therefore, the PI controller regulates the PV voltage during active charging, while the supervisory switch determines whether the converter is permitted to continue transferring energy to the battery.

The PI controller parameters used in the simulation are summarized in Table 2.

Table 2. PI Controller Parameters

No	Parameter	Value
1	Controller type	PI
2	Controller form	Parallel
3	Time domain	Continuous-time
4	Proportional gain, V_{MP}	−0.0397534768249176
5	Integral gain, I_{MP}	−5.18190685384352
6	Lower saturation limit	0.05
7	Upper saturation limit	0.95
8	Tuning method	Transfer Function Based (PID Tuner App)

Table 2 presents the PI controller parameters used to regulate the system response. The controller type is set to PI (Proportional-Integral), which combines proportional and integral actions to reduce the difference between the reference value and the actual output. The controller form is parallel, meaning that the proportional and integral components operate independently and their outputs are combined to produce the controller signal. The controller uses a continuous-time domain, indicating that the PI control algorithm is designed to operate continuously rather than in a discrete sampling-based form.

The proportional gain (V_{MP}) is set to -0.0397534768249176, while the integral gain (I_{MP}) is set to -5.18190685384352. The proportional gain determines the controller's immediate response to the error, whereas the integral gain accumulates the error over time to eliminate steady-state error. The negative values of both gains indicate that the controller action is configured according to the direction or polarity of the controlled system. The lower saturation limit is set to 0.05, while the upper saturation limit is 0.95. These limits constrain the controller output within the range of 0.05–0.95, preventing the control signal from exceeding the allowable operating range of the system.

Finally, the PI controller parameters are obtained using a Transfer Function Based tuning method through the PID Tuner App. This method uses the system's transfer function to determine suitable controller gains so that the desired dynamic response and stability can be achieved. Overall, the parameters in Table 2 define the PI controller configuration and limit its output to ensure appropriate and stable control performance.

2.4. Coloum Counting

The battery is used as the energy storage element at the output of the buck converter. The battery model has a nominal capacity of 100 Ah, an initial SOC of 99.99%, and a charging voltage limit of 12.6 V. Battery current and voltage are continuously monitored to estimate the SOC and determine the charging condition.

SOC estimation is performed using the Coulomb Counting method, which estimates the change in battery SOC from the accumulated battery current over time. The SOC estimation equation used in the simulation is given by:

$$SOC(k) = SOC(k-1) + \frac{I_{ch}(k)\Delta t}{Q_n} \times 100\% \quad (9)$$

The current sign convention follows the implementation of the battery model in Simulink. The estimated SOC and battery voltage are then supplied to the supervisory switch controller. During the charging

ISSN: 2715-6427

state, the charging command is enabled when the SOC remains below the full-charge threshold and the battery voltage is below the specified charging voltage limit:

$$SOC < 100\% \;\; and \;\; V_{bat} < 12.6\,V \tag{10}$$

When the SOC reaches 100% or the battery voltage reaches 12.6 V, the supervisory controller disables the charging command by blocking the PWM control signal. To prevent repeated switching around the full-charge condition, a hysteresis threshold is applied. After cut-off, charging is permitted again when the SOC decreases to 95% and the battery voltage remains below the specified charging limit:

$$SOC \leq 95\% \tag{11}$$

Thus, the Coulomb Counting method is used specifically for SOC estimation, while the estimated SOC and battery voltage are used by the supervisory controller to determine the charging enable, cut-off, and restart conditions. During active charging, the P&O MPPT and PI controller continue to regulate the PV operating point and the buck converter duty cycle. When a cut-off condition is reached, the supervisory controller overrides the normal charging command and disables the PWM command.

3. RESULTS AND DISCUSSION

This section presents and discusses the simulation results of the proposed PV battery charging regulation system. The evaluation focuses on the battery State of Charge (SOC), charging current, duty-cycle response, PV operating conditions, and buck converter voltage response. The results are analyzed to evaluate the interaction between the P&O MPPT algorithm, PI controller, buck converter, and Coulomb Counting-based supervisory charging control.

The overall simulation performance is summarized in Table 3. The values are obtained from the simulation responses presented in Figures 6–9.

Table 3. Summary of Simulation Performance

No	Parameter	Simulation Result	Operating Condition
1	Initial battery voltage	11.4 V	Beginning of simulation
2	Battery voltage during charging	11.90 V	Normal charging
3	Battery current	−11 A to −7 A	Active charging
4	Final battery current	0 A	After charging cut-off
5	Initial SOC	99.99%	Beginning of observation
6	Full SOC	100%	3.45 s
7	PV voltage	29 V	Normal operating condition
8	PV current	7.5 A	Normal operating condition
9	PV power	210 W	Normal operating condition
10	Reduced PV power	120 W	Changed PV condition
11	PV voltage at cut-off	33 V	Charging disabled
12	Duty cycle	0.5	Normal charging
13	Duty cycle at cut-off	0	Charging disabled
14	Battery charging voltage limit	12.6 V	Supervisory limit

The results indicate that the proposed control structure coordinates the PV-side MPPT and voltage regulation with the battery-side charging supervision. During normal charging, the P&O algorithm determines the PV voltage reference, while the PI controller adjusts the buck converter duty cycle to regulate the PV operating voltage. When the battery reaches the defined full-charge condition, the supervisory controller disables the charging command, resulting in a duty cycle of zero and a battery charging current of 0 A.

3.1 Coulomb Counting-Based SOC Evaluation

The performance of battery charging is evaluated based on voltage, current, and State of Charge (SOC) estimated using the Coulomb Counting method, as shown in Figure 6. This method calculates the accumulation of current over time to monitor SOC changes during the charging process.

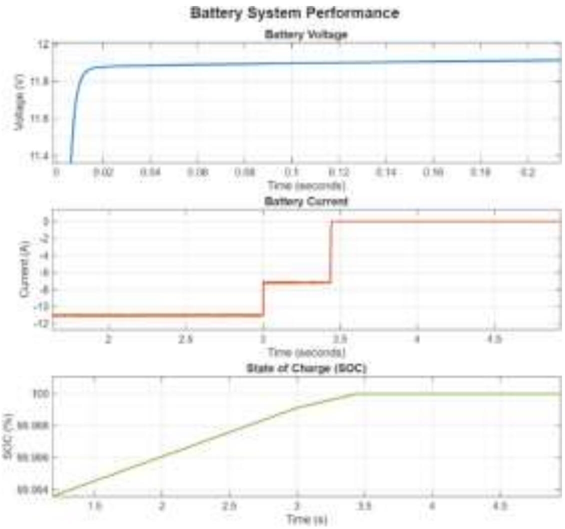

Figure 6. Coulomb Counting-Based SOC Evaluation

At the beginning of the observation (0–0.22 s), the battery voltage rapidly increased from around 11.4 V to 11.88 V, then rose slowly and stabilized around 11.90 V. Between 1.5–5 s, the battery current was around −11 A and then decreased to −7 A at around 3 s, as the SOC increased from around 99.99% to 100%. The SOC reached 100% at around 3.4–3.5 s and then remained constant. At around 3.45 s, the battery current dropped from −7 A to 0 A after the SOC reached 100%. This condition indicates that the SOC estimation based on Coulomb Counting is integrated with switch control, where reaching full SOC serves as the basis for activating the charging cut-off.

3.2 Duty Cycle Testing Under Various SOC Conditions

The duty cycle response was analyzed to see the relationship between the battery charging condition and the buck converter control signal, as shown in Figure 7. At the beginning of the simulation, the duty cycle increased to around 0.5, then remained relatively stable with small fluctuations until it approached 3.45s.

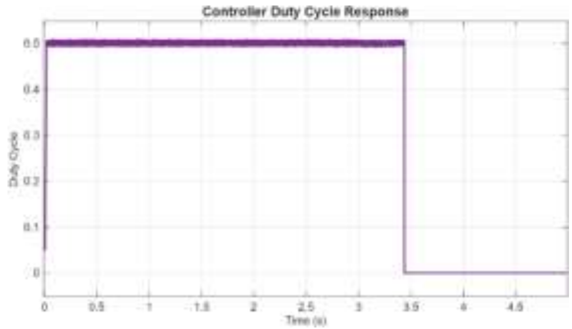

Figure 7. Duty Cycle Testing Under Various SOC Conditions

The relatively stable duty cycle around 0.5 indicates that the system is still in a normal charging condition and the buck converter continues to operate to transfer energy from the PV to the battery. At around 3.45 s, the duty cycle drops from around 0.5 to 0 and remains at that level until the end of the simulation. This change occurs simultaneously with the SOC reaching 100% and the battery current becoming 0 A, indicating that the charging cut-off has been activated by the switch control. The results show the relationship between SOC and duty cycle: as long as the SOC has not reached the full limit, the duty cycle continues to be used to support the charging process, whereas when the SOC reaches 100%, the switch control changes the duty cycle to 0 to end the charging process.

3.3 MPPT Testing of PV Systems

The performance of Maximum Power Point Tracking (MPPT) is analyzed based on the response of voltage, current, and PV power over time, as shown in Figure 8. These three parameters are used to observe changes in the PV operating point during normal conditions, changes in source conditions, and when the system enters the charging cut-off condition.

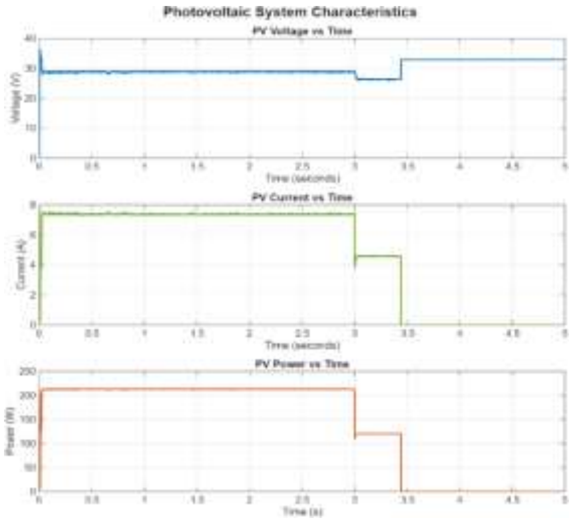

Figure 8. MPPT Testing on PV

At the beginning of the simulation, the PV voltage experienced a transient before reaching around 28–29 V, with a current of about 7.5 A and a power of around 210 W. This condition remained relatively stable until about 3 seconds, indicating that the PV operating point could be maintained during the initial period. At around 3 seconds, the PV voltage and current decreased to approximately 26–27 V and 4.5 A, respectively, causing the power to drop to around 120 W. This condition indicated a change in the PV operating point, which was then followed by adjustments from the MPPT controller.

This condition persisted until close to 3.4 seconds with lower power. Subsequently, at around 3.4–3.5 seconds, the PV voltage increased to about 33 V, while the PV current and power dropped to 0 A. This condition indicated the cessation of energy transfer from the PV and was consistent with the duty cycle reduction from about 0.5 to 0 in Figure 7. Thus, the charging cut-off causes the buck converter to stop supplying energy to the battery.

3.4 Buck Converter Testing

The performance of the buck converter is evaluated based on the input and output voltage response over time, as shown in Figure 9. This analysis aims to assess the converter's ability to reduce the PV voltage and produce the appropriate voltage during the battery charging process.

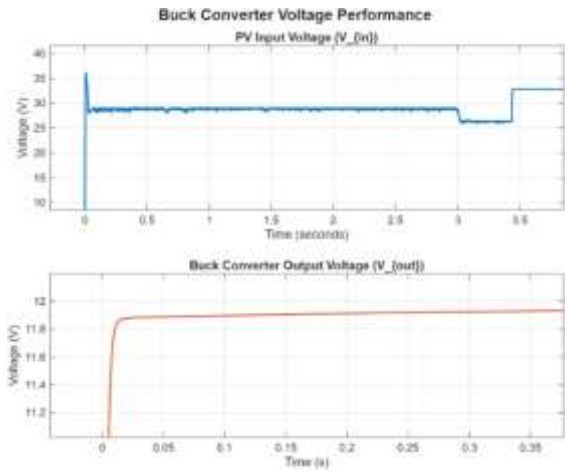

Figure 9. Buck Converter Testing

On the input side, the PV voltage experiences a transient up to around 36 V before dropping and stabilizing in the range of 28–29 V for about 3 seconds. At around 3 seconds, the input voltage decreases to 26–27 V, then increases to around 33 V toward 3.4–3.5 seconds as the system enters the charging cut-off condition. This change corresponds with the duty cycle dropping to zero. On the output side, the voltage increases from around 11.0 V to 11.88 V in about 0.02 seconds, then gradually rises to around 11.9 V by the end of the observation interval.

This shows that the buck converter is capable of reducing the higher PV voltage to an output voltage suitable for the battery charging process. The difference between the input voltage of around 28–29 V and the output voltage of around 11.9 V indicate the function of the buck converter as a conversion stage between the PV and the battery. During the charging process, a duty cycle of around 0.5 maintains the conversion process, while at cut-off, the duty cycle becomes zero, cut off the energy transfer to the battery.

4. CONCLUSION

This study successfully developed and evaluated a simulation-based solar charging regulator that coordinates MPPT, closed-loop buck converter control, and SOC-based charging supervision. The proposed system was able to regulate the PV operating point during the charging process and automatically terminate the charging command when the battery reached the defined full-charge condition.

The simulation results show that during normal charging, the buck converter operates with a duty cycle of approximately 0.5, while the battery charging current remains in the range of approximately -11 A to -7 A. Starting from a near-full initial SOC condition, the estimated battery SOC reaches 100% at approximately 3.45 s. At this condition, the supervisory controller reduces the duty cycle from approximately 0.5 to 0, causing the battery charging current to decrease to 0 A and thus automatically disabling the charging command. These results demonstrate that the proposed control structure can coordinate PV power extraction, converter regulation, and battery charging supervision within a single charging system.

Overall, the proposed system demonstrates the feasibility of using SOC-based supervisory control to determine the continuation or termination of PV-to-battery charging while maintaining MPPT and closed-loop voltage regulation during normal operation. The results provide a basis for further development and experimental validation using hardware implementation under varying irradiation, temperature, and battery operating conditions.

ACKNOWLEDGEMENTS

The author expresses gratitude to Universitas PGRI Adi Buana Surabaya for the support and facilities provided during the implementation of this research. That support has helped the author in the process of design, simulation, and completion of the research.

REFERENCES

[1] J. D. Bastidas-Rodriguez, E. Franco, G. Petrone, C. A. Ramos-Paja, and G. Spagnuolo, “Maximum power point tracking architectures for photovoltaic systems in mismatching conditions: a review,” *IET Power Electronics*, vol. 7, no. 6, pp. 1396–1413, Jun. 2014, doi: 10.1049/iet-pel.2013.0406.

[2] T. Esram and P. L. Chapman, “Comparison of Photovoltaic Array Maximum Power Point Tracking Techniques,” *IEEE Transactions on Energy Conversion*, vol. 22, no. 2, pp. 439–449, Jun. 2007, doi: 10.1109/TEC.2006.874230.

[3] B. Subudhi and R. Pradhan, “A Comparative Study on Maximum Power Point Tracking Techniques for Photovoltaic Power Systems,” *IEEE Trans. Sustain. Energy*, vol. 4, no. 1, pp. 89–98, Jan. 2013, doi: 10.1109/TSTE.2012.2202294.

[4] R. Alik, A. Jusoh, and T. Sutikno, “A Review on Perturb and Observe Maximum Power Point Tracking in Photovoltaic System,” *TELKOMNIKA (Telecommunication Computing Electronics and Control)*, vol. 13, no. 3, p. 745, Sep. 2015, doi: 10.12928/telkomnika.v13i3.1439.

[5] W. Xiao, N. Ozog, and W. G. Dunford, “Topology Study of Photovoltaic Interface for Maximum Power Point Tracking,” *IEEE Transactions on Industrial Electronics*, vol. 54, no. 3, pp. 1696–1704, Jun. 2007, doi: 10.1109/TIE.2007.894732.

[6] M. Fulczyk and J. Bertsch, “Ground-fault currents in unit-connected generators with different elements grounding neutral,” *IEEE Transactions on Energy Conversion*, vol. 17, no. 1, pp. 61–66, Mar. 2002, doi: 10.1109/60.986438.

[7] R. W. Erickson and D. Maksimović, *Fundamentals of Power Electronics*. Boston, MA: Springer US, 2001. doi: 10.1007/b100747.

[8] W.-Y. Chang, “The State of Charge Estimating Methods for Battery: A Review,” *ISRN Applied Mathematics*, vol. 2013, pp. 1–7, Jul. 2013, doi: 10.1155/2013/953792.

[9] A.M.S.M.H.S.Attanayaka, J.P.Karunadasa, and K.T.M.U.Hemapala, “Estimation of state of charge for lithium-ion batteries - A Review,” *AIMS Energy*, vol. 7, no. 2, pp. 186–210, 2019, doi: 10.3934/energy.2019.2.186.

[10] K. Movassagh, A. Raihan, B. Balasingam, and K. Pattipati, “A Critical Look at Coulomb Counting Approach for State of Charge Estimation in Batteries,” *Energies (Basel).*, vol. 14, no. 14, p. 4074, Jul. 2021, doi: 10.3390/en14144074.

[11] K. Movassagh, A. Raihan, B. Balasingam, and K. Pattipati, “A Critical Look at Coulomb Counting Approach for State of Charge Estimation in Batteries,” *Energies (Basel).*, vol. 14, no. 14, p. 4074, Jul. 2021, doi: 10.3390/en14144074.

[12] L. Ling, D. Sun, X. Yu, and R. Huang, “State of charge estimation of Lithium-ion batteries based on the probabilistic fusion of two kinds of cubature Kalman filters,” *J. Energy Storage*, vol. 43, p. 103070, Nov. 2021, doi: 10.1016/j.est.2021.103070.

[13] S. Saravanan and N. Ramesh Babu, “Maximum power point tracking algorithms for photovoltaic system – A review,” *Renewable and Sustainable Energy Reviews*, vol. 57, pp. 192–204, May 2016, doi: 10.1016/j.rser.2015.12.105.

[14] P. Joshi and S. Arora, “Maximum power point tracking methodologies for solar PV systems – A review,” *Renewable and Sustainable Energy Reviews*, vol. 70, pp. 1154–1177, Apr. 2017, doi: 10.1016/j.rser.2016.12.019.

[15] J. P. Ram, T. S. Babu, and N. Rajasekar, “A comprehensive review on solar PV maximum power point tracking techniques,” *Renewable and Sustainable Energy Reviews*, vol. 67, pp. 826–847, Jan. 2017, doi: 10.1016/j.rser.2016.09.076.

[16] M. A. M. Ramli, S. Twaha, K. Ishaque, and Y. A. Al-Turki, “A review on maximum power point tracking for photovoltaic systems with and without shading conditions,” *Renewable and Sustainable Energy Reviews*, vol. 67, pp. 144–159, Jan. 2017, doi: 10.1016/j.rser.2016.09.013.

[17] M. A. Hannan, M. S. H. Lipu, A. Hussain, and A. Mohamed, “A review of lithium-ion battery state of charge estimation and management system in electric vehicle applications: Challenges and recommendations,” *Renewable and Sustainable Energy Reviews*, vol. 78, pp. 834–854, Oct. 2017, doi: 10.1016/j.rser.2017.05.001.

[18] B. Hauke, “Basic Calculation of a Buck Converter’s Power Stage,” 2011. [Online]. Available: www.ti.com

[19] J. Ahmed and Z. Salam, “An improved perturb and observe (P&O) maximum power point tracking (MPPT) algorithm for higher efficiency,” *Appl. Energy*, vol. 150, pp. 97–108, Jul. 2015, doi: 10.1016/j.apenergy.2015.04.006.

[20] A. I. M. Ali and H. R. A. Mohamed, “Improved P&O MPPT algorithm with efficient open-circuit voltage estimation for two-stage grid-integrated PV system under realistic solar radiation,” *International Journal of Electrical Power & Energy Systems*, vol. 137, p. 107805, May 2022, doi: 10.1016/j.ijepes.2021.107805.

[21] N. Mohammed and A. M. Saif, “Programmable logic controller based lithium-ion battery management system for accurate state of charge estimation,” *Computers & Electrical Engineering*, vol. 93, p. 107306, Jul. 2021, doi: 10.1016/j.compeleceng.2021.107306.

[22] M. Kamran, M. Mudassar, M. R. Fazal, M. U. Asghar, M. Bilal, and R. Asghar, “Implementation of improved Perturb & Observe MPPT technique with confined search space for standalone photovoltaic system,” *Journal of King Saud University - Engineering Sciences*, vol. 32, no. 7, pp. 432–441, Nov. 2020, doi: 10.1016/j.jksues.2018.04.006.